

## Cosmic Microwave Background Anisotropy Induced by Cosmic Strings on Angular Scales $\gtrsim 15'$

B. Allen,<sup>1</sup> R. R. Caldwell,<sup>2</sup> S. Dodelson,<sup>3</sup> L. Knox,<sup>4</sup> E. P. S. Shellard,<sup>5</sup> and A. Stebbins<sup>3</sup>

<sup>1</sup>Department of Physics, University of Wisconsin—Milwaukee, P.O. Box 413, Milwaukee, Wisconsin 53201

<sup>2</sup>Department of Physics and Astronomy, University of Pennsylvania, Philadelphia, Pennsylvania 19106

<sup>3</sup>NASA/Fermilab Astrophysics Center, P.O. Box 500, Batavia, Illinois 60510

<sup>4</sup>Canadian Institute for Theoretical Astrophysics, Toronto, Ontario, Canada M5S 3H8

<sup>5</sup>University of Cambridge, D.A.M.T.P. Silver Street, Cambridge CB3 9EW United Kingdom

(Received 5 May 1997)

We have computed an estimate of the angular power spectrum of the cosmic microwave background induced by cosmic strings on angular scales  $\gtrsim 15'$ , using a numerical simulation of a cosmic string network and have decomposed this pattern into scalar, vector, and tensor parts. The anisotropies from vector modes dominate except on very small angular scales, and we find no evidence for strong acoustic oscillations in the scalar anisotropy. The anisotropies generated after recombination are even more important than in adiabatic models. The total anisotropy on small scales is inconsistent with current measurements. The calculation has a number of uncertainties, the largest of which is due to finite temporal range. [S0031-9007(97)04228-2]

PACS numbers: 98.70.Vc, 98.80.Cq

The spectrum of cosmic microwave background (CMB) anisotropy on the angular scales somewhat smaller than that subtended by the horizon at last scattering provides a powerful probe of the nature of inhomogeneities and matter in our universe [1]. On these scales hydrodynamical effects can leave characteristic signatures of adiabatic or isocurvature perturbations [2], active or passive perturbations [3], an open or closed universe, or even a high or low Hubble constant. Cosmic strings are topological defects which may have formed in the very early Universe and may be responsible for the formation of large scale structure observed in the Universe today [4]. While cosmic string induced perturbations are clearly both isocurvature and active the interplay between these two properties allows a range of possible behavior for the degree scale anisotropy [5]. One method for determining the signature for cosmic strings is via simulation, i.e., by numerically evolving a network of cosmic strings in a simulated universe and computing the pattern of anisotropy they would produce. We present the results of just such a calculation in this Letter. While we have not explored the full range of cosmological parameters, or included all the effects on network dynamics, our results are suggestive of what is and is not important for small scale anisotropies from the cosmic string model.

*Methodology.*—Cosmic strings only interact gravitationally with the rest of the matter and produce only small metric perturbations. Thus we may ignore back-reaction of the metric perturbations on the strings and solve for the evolution of the string network in an unperturbed cosmology. This “stiff-source” approximation allows us to do the string simulation and later compute the perturbations to the matter. It also allows us to reuse the same string simulation to compute the perturbations in cosmologies with different matter content. Here we have reused one

of the simulations that was used in Allen *et al.* [6]. While that simulation took the size of the simulation box to be twice the present day horizon, we may use the assumption of self-similar evolution of the string network (“scaling”) to rescale the box to a smaller size while simultaneously decreasing both the starting and ending time of the simulation. The equations of motion of the strings will still be satisfied so long as the cosmological expansion remains a power law, which in this case is  $a \propto t^{\frac{2}{3}}$ , corresponding to a flat Friedmann-Robertson-Walker matter dominated universe. These simulations should not be used for epochs too close to matter-radiation equality, which means that if we want to study the effects close to recombination we should really only consider a large Hubble constant which puts recombination long after matter-radiation equality. Here we use  $H_0 = 80$ , but even with this Hubble constant the effects of the matter-radiation transition are liable to be significant, and below we discuss what these effects are liable to be. Throughout we take the baryon fraction  $\Omega_b = 0.02$  to be consistent with the predictions of nucleosynthesis.

The cosmic string simulation is in a cubical box whose comoving size we denote by  $L$ . The initial time step, when the comoving horizon ( $\equiv$  conformal time) is given by  $\eta_i = 0.05L$ , after which the string network rapidly relaxed to its scaling configuration by the time  $\eta = 0.055L$ . The simulation ends at  $\eta_f = 0.5L$ . During this period the Universe has grown by a factor of 100. In order to use this simulation to compute small-scale anisotropies produced near recombination one must make the measurement of the anisotropies long after the end of the string simulation. One may do this by rescaling the simulation to end just after recombination, but continuing to propagate the brightness pattern unperturbed through the periodic box until today. This *free-streaming* procedure

will lead to a brightness pattern which is quasiperiodic on the sky, the size of the periodic patches being the angle subtended by length  $L$  when placed at the distance of the surface of last scattering. We expect that the statistical properties of the pattern in each of these patches will be nearly the same as for a similar sized patch in an infinite nonperiodic universe.

Since the metric perturbations are small we may use the linearized Einstein equations for the metric and the linearized Boltzmann equation for the anisotropies. This makes the equations for the temperature anisotropy linear in the stress energy of the strings,  $\Theta_{\mu\nu}$ . The dynamics of the strings is described by nonlinear equations, and leads to the non-Gaussian distribution for  $\Theta_{\mu\nu}$ , but the *response* of the photons to the strings is linear. The solution of the linear equations may be written as a homogeneous and inhomogeneous part

$$\begin{aligned} \frac{\Delta T}{T}(\hat{\mathbf{n}}, \mathbf{x}_{\text{obs}}, \eta_{\text{obs}}) &= \left(\frac{\Delta T}{T}\right)^{\text{I}} + \int d\eta' \int d^3\mathbf{x}' \\ &\times D^{\mu\nu}(\hat{\mathbf{n}}, \mathbf{x}, \mathbf{x}', \eta, \eta') \\ &\times \Theta_{\mu\nu}(\mathbf{x}'\hat{\mathbf{n}}'), \end{aligned} \quad (1)$$

where  $(\frac{\Delta T}{T})^{\text{I}}$  depends on the initial condition for the cosmological fluids (cold, dark matter, baryons, photons, and neutrinos) which is often referred to as *compensation*. We have compensated the strings with adiabatic perturbations in the other matter so as to make the total density initially uniform, just as in Ref. [6]. Clearly this is not exactly the correct prescription except on superhorizon scales. Nevertheless we find that  $(\frac{\Delta T}{T})^{\text{I}}$  is small in comparison with the second term (this is consistent with the results of Ref. [7]). We think this is likely to remain true with different prescriptions for compensation.

The way we have used Eq. (1) is somewhat different than has typically been done in the past. Rather than concentrating on a few  $\mathbf{x}_{\text{obs}}$  we will effectively compute the entire brightness pattern throughout the simulation box. This function of the 5D phase space  $(\hat{\mathbf{n}}, \mathbf{x}_{\text{obs}})$  would require an unpractical amount of computer memory. One can reduce the memory requirement by Fourier decomposing the  $\mathbf{x}$  dependence and then, for each  $\mathbf{k}$  mode, expanding the  $\hat{\mathbf{n}}$  dependence in spherical harmonics,  $Y_{(l,m)}$ , using a spherical polar coordinate system with the pole in the direction of  $\mathbf{k}$ . The beauty of this decomposition is that the  $m = 0$  terms correspond to scalar modes, the  $m = \pm 1$  terms to vector modes, and the  $m = \pm 2$  to tensor modes [8]. Modes with  $|m| > 2$  are zero since they are not coupled to the gravitational field (in linear theory) and may be ignored. From the mode coefficients,  $\Delta_{(l,m)}(\mathbf{k})$ , one may construct the volume average of the  $C_l$ 's measured by all the observers in the box:

$$\overline{C}_l = \overline{C}_l^{\text{S}} + \overline{C}_l^{\text{V}} + \overline{C}_l^{\text{T}}, \quad (2)$$

where

$$\begin{aligned} \overline{C}_l^{\text{S}} &= \frac{1}{(2l+1)L^3} \sum_{\mathbf{k}} |\Delta_{(l,0)}|^2, \\ \overline{C}_l^{\text{V}} &= \frac{1}{(2l+1)L^3} \left( \sum_{\mathbf{k}} |\Delta_{(l,+1)}|^2 + |\Delta_{(l,-1)}|^2 \right), \\ \overline{C}_l^{\text{T}} &= \frac{1}{(2l+1)L^3} \left( \sum_{\mathbf{k}} |\Delta_{(l,+2)}|^2 + |\Delta_{(l,-2)}|^2 \right). \end{aligned} \quad (3)$$

There are no cross terms between different terms because all of the modes are orthogonal [9]. Applying this decomposition to the right-hand side of Eq. (1) induces a scalar-vector-tensor decomposition of  $D^{\mu\nu}$  and  $\Theta_{\mu\nu}$ . We may perform the decomposition of  $\Theta_{\mu\nu}$  numerically. The corresponding components of  $D^{\mu\nu}$  are solutions of the linearized Einstein-Boltzmann equation which we have computed numerically using standard techniques [10].

*Tests.*—Our calculation has three parts: the string simulation, the numerical calculation of the Green functions, and the computation of the brightness perturbation, which merges the two preceding parts. A number of tests have been made on the simulation [6,7,11], which we do not discuss here.

The Green functions have been tested in two ways. First, the code which computes the scalar and tensor Green functions [10] has been used to determine the angular power spectrum for a model with adiabatic perturbations only. These calculations agree to within a percent with standard results. Although the vector Green functions cannot be tested in this way, there is an analytic approximation in terms of spherical Bessel functions, which holds after recombination. For this case, there is excellent agreement between the analytic and numerical results. Similarly, the scalar Green functions have been tested on large scales by comparing with analytic approximations; again we find excellent agreement.

To test the full pipeline of merging the Green functions with the stress energies, we calculated the anisotropies in a matter dominated universe with one domain wall [12]. The  $C_l$ 's in this case can be calculated analytically. The numerical results are in very good agreement with the exact results.

The greatest limitation of our ability to accurately compute the small angle CMB anisotropy is the lack of dynamic range of the cosmic string simulation. Although the simulation runs over a range of 10 in conformal time, this is insufficient to accurately follow the evolution of modes from well outside to inside the horizon, where they begin to oscillate. Our results indicate that modes well inside the horizon make a significant contribution to the anisotropy. As an example, when  $\eta \sim 6/k$ , the traceless part of  $|\Theta_{\mu\nu}|^2$  is half its maximum value.

Because of the limited spatial resolution of the cosmic string simulation, a limited number of Fourier modes of the source stress energy are available. To determine whether this would prevent us from seeing ‘‘Doppler peaks,’’ we used the same number of modes over the same

range of time for a model with adiabatic initial conditions, for which the exact results are known. Qualitative agreement was obtained, as the peak structure and location were clearly evident. Hence, we do not expect that the limited spatial resolution should prevent us from resolving features in the angular power spectrum. Finite grid effects lead to an artificial drop of only  $\sim 10\%$  in the amplitude of the angular power spectrum for the largest  $l$  values obtained from a simulation volume.

Finally, we have used the same simulation to calculate anisotropies generated at different times. However, we do not expect there to be strong correlations in either the source stress energy or the anisotropy on time intervals longer than the run time of the string simulation. Hence, we do not expect the recycling of the numerical simulation to have a strong effect on our results.

**Results.**—We obtain the final angular power spectrum,  $C_l$ , by combining the results from different rescalings of the results of the cosmic string numerical simulation. As discussed earlier, we exploit the scaling properties of the string network to make up for the finite temporal dynamic range of the simulation. For multipole moments in the range  $2 < l < 20$  (large angles) we use one box, covering the redshift range  $0 < z < 100$ . For  $100 < l < 800$  (small angles) we use two different boxes corresponding to  $700 < z < 17\,000$  and  $60 < z < 700$ .

Our results are shown in Figs. 1 and 2. On large angular scales, we see that the dominant source of the anisotropy is due to vector perturbations. This is an important result, as it means the COBE normalization of the mass per unit length is determined mainly by the amplitude of the vector, not scalar, spectrum.

We may use the large angle results as a test of our techniques, by comparing with the results of Ref. [6], which used the same simulation. They found  $l(l+1)C_l \sim 350(G\mu)^2$  at large angles, so our results are a

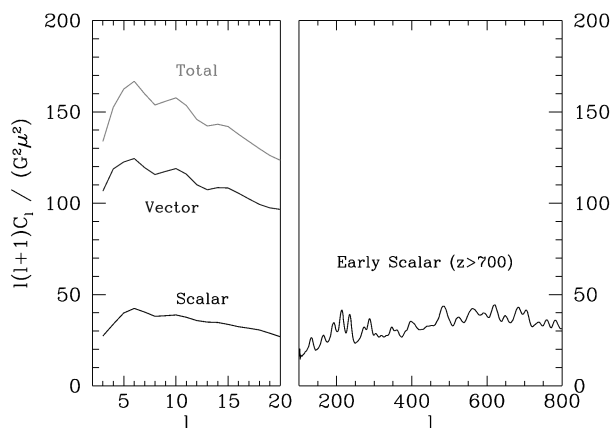


FIG. 1. Angular power spectrum at large and small scales for the cosmic string simulation. Tensors do not contribute appreciably. On small scales only the contribution from early times ( $z > 700$ ) can be calculated reliably over the full range of angular scales.

factor of  $\sim 2.8$  smaller. However, we are in accord with the shape of the spectrum and the determination that the majority of the large angle anisotropy is generated at redshifts  $z \lesssim 20$  (as in Fig. 3 of Ref. [6]). When normalizing to COBE [13], we find  $\mu_6 \equiv G\mu \times 10^6 = 1.7$ , a factor  $\sim \sqrt{2.8}$  higher than that of Ref. [6]. This result is comparable with  $\mu_6 = 1.5(\pm 0.5)$  [14],  $1.7(\pm 0.7)$  [15], and 2 [16]. Thus, our large angle normalization falls in the middle of the range spanned by other calculations.

On small angular scales Fig. 1 shows the contribution to the scalar  $C_l$ 's from early times ( $z > 700$ ). There is a gradual rise in the spectrum from  $l = 100$  till a very broad plateau for  $l \gtrsim 200$ . The increase is less than a factor of 2 so may not be significant.

Calculating the contribution from the vector modes and from the late time contributions to the scalar modes presents a problem. In each case, the box size must be chosen to be very large in order to get to very late times. The smallest scales ( $l \gtrsim 300$ ) therefore become unreliable. In Fig. 2, we show the results for  $100 < l < 300$ . The most striking feature here is that both the vector contribution and the late time scalar contribution are larger than the early time scalars. The net result is that the mild acoustic peak in the scalar spectrum becomes hidden. The total spectrum therefore is quite flat. (It is unclear if the slight drop in the total is significant.) While these qualitative features appear to be robust, we believe that in future work they will be subject to quantitative changes which will tend to boost power on small-angular scales.

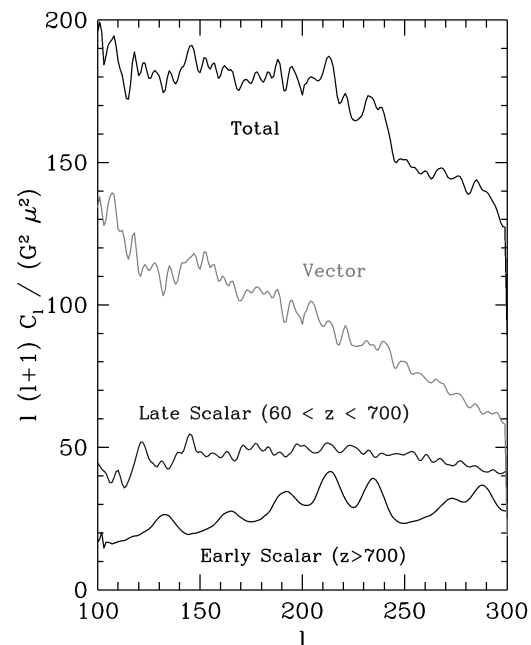


FIG. 2. Angular power spectrum at small scales for the cosmic string simulation. The three different contributions are the early time scalars, late time scalars, and vectors. These add incoherently to give the total spectrum.

*Discussion.*—We have calculated the anisotropies in the CMB and the perturbations to matter induced by a network of cosmic strings in the matter era. This calculation uses *all* the components of the stress-energy tensor and exact Green functions for all modes. The greatest source of uncertainty in our results is due to the limited spatial resolution and run time of the numerical simulation.

On large scales, we find that the vector perturbations are very important for the CMB anisotropy from cosmic strings. Our results for anisotropies at small scales are too low to be consistent with current measurements. Future work will determine the effects of a radiation-matter transition in the cosmic string simulation, in which the long string density and rms velocity relaxes from the radiation- to matter-era scaling values, inclusion of a “wiggly” equation of state for the cosmic strings, or a lower value of the Hubble parameter and a larger value of the baryon density can boost the small-scale power sufficiently. Since vectors dominate, even if any of these effects do raise the early time scalar spectrum by as much as a factor of 2, the total power would only go up by 20%. Even if a primary Doppler peak were to become a more prominent feature, this work suggests that secondary Doppler peaks are not anticipated in cosmic string models. Finally let us mention that qualitatively similar results have also been found for global defects [17].

The work of B.A. was supported by NSF Grants No. PHY91-05935 and No. PHY95-07740. The work of R.R.C. was supported by DOE Grant No. DOE-EY-76-C-02-3071. The work of S.D. and A.S. was supported in part by DOE and NASA Grant No. NAGW-2788 at Fermilab. E.P.S. is partially supported by PPARC Grant No. GR/H71550.

- [1] See, e.g., S. Dodelson, astro-ph/9702134, 1997.
- [2] W. Hu and N. Sugiyama, Phys. Rev. D **51**, 2599 (1995).
- [3] R.G. Crittenden and N.G. Turok, Phys. Rev. Lett. **75**, 2642 (1995); A. Albrecht, D. Coulson, P. Ferreira, and J. Magueijo, Phys. Rev. Lett. **76**, 1413 (1996); N. Turok, Phys. Rev. D **54**, 3686 (1996); W. Hu, D.N. Spergel, and M. White, Phys. Rev. D **55**, 3288 (1997).
- [4] A. Vilenkin, Phys. Rep. **121**, 263 (1985); A. Vilenkin and E.P.S. Shellard, *Cosmic Strings and other Topological Defects* (Cambridge University Press, Cambridge, England, 1994); M. Hindmarsh and T.W.B. Kibble, Rep. Prog. Phys. **58**, 47 (1995).
- [5] J. Magueijo, A. Albrecht, D. Coulson, and P. Ferreira, Phys. Rev. Lett. **76**, 2617 (1996); J. Magueijo, A. Albrecht, P. Ferreira, and D. Coulson, Phys. Rev. D **54**, 3727 (1996).
- [6] B. Allen, R.R. Caldwell, E.P.S. Shellard, A. Stebbins, and S. Veeraraghavan, Phys. Rev. Lett. **77**, 3061 (1996).
- [7] B. Allen *et al.* (to be published).
- [8] L.F. Abbott and R.K. Schaefer, Astrophys. J. **308**, 546 (1986).
- [9] A. Stebbins and S. Dodelson, astro-ph/9705177, 1997.
- [10] The scalar part of the Boltzmann code is based on S. Dodelson and J.M. Jubas, Phys. Rev. Lett. **70**, 2224 (1993); the tensor part on S. Dodelson, L. Knox, and E. Kolb, Phys. Rev. Lett. **72**, 3444 (1994); while the vector part is new and was developed by Knox and Dodelson.
- [11] B. Allen and E.P.S. Shellard, Phys. Rev. Lett. **64**, 119 (1990).
- [12] S. Veeraraghavan and A. Stebbins, Astrophys. J. **395**, L55 (1992).
- [13] G.P. Smoot *et al.*, Astrophys. J. **396**, L1 (1992).
- [14] D. Bennett, A. Stebbins, and F. Bouchet, Astrophys. J. Lett. **399**, L5 (1992).
- [15] L. Perivolaropoulos, Phys. Lett. B **298**, 305 (1993).
- [16] D. Coulson, P. Ferreira, P. Graham, and N. Turok, Nature (London) **368**, 27 (1994).
- [17] U. Pen, U. Seljak, and N. Turok (private communication).